Optimum heating of pressure elements

J. Taler

Institute of Process and Power Engineering,
Cracow University of Technology,
al. Jana Pawła II 37,
31-864 Cracow,
Poland

Abstract

Five different methods for determining optimum fluid temperature changes during heating or cooling thick plate are examined. The first method presented in this paper is based on the discrete form of Duhamel's integral. The method can be easily applied to bodies of complex shapes and is recommended for use, while three other methods: the Laplace Transform, Burggraf analytical method, and space marching method can be applied to only a very limited number of optimum control problems. In the fifth approach, the optimum fluid temperature changes are approximated by a function with unknown parameters, which are determined using the least squares method.

These five techniques were used to determine time changes of fluid temperature assuring linear increase of the slab wall temperature at the given location inside the body. No one approach is perfect. The optimum fluid temperature changes are burdened with a large uncertainty at the beginning of the heating process.

1. Introduction

      Large thermal stresses can occur at the inner surface of thick walled pressure components of steam boilers during the start-up and shut-down operations. Measurements of strains or stresses on the inner component surface, which is exposed to hot fluid under high pressure, is extremely difficult. For this reason, the thermal stresses at the inner surface are monitored indirectly by measurements of time variations of the component wall temperature at the interior location or at the outer thermally insulated surface, which are easily accessible. From the solution of the inverse heat conduction problem (IHCP) the spatial temperature distribution in the whole component for any time is determined.

In computer monitoring systems used in power plants, the time-space temperature and stress distribution in the pressure components is calculated sequentially in an on-line mode in order to inform the operator or the control system to take measures to speed up or slow down the start-up or shutdown process.

Determination of optimum fluid temperature changes is also an inverse heat conduction problem. To avoid excess thermal stresses, the temperature of the component wall should be increased or decreased according to the prescribed function of time. Another option is to adjust the fluid temperature changes in such a way that the thermal stress at the point of stress concentration does not exceed the allowable values.

With the exception of the earliest time period, the optimum rate of fluid and wall temperature changes is constant, if the physical properties of the component material and allowable stress are constant. This optimum rate of fluid temperature changes can easily be determined based on the quasi-steady state theory. However, determininig fluid temperature changes at the earliest time of the transient process, which assure that the calculated temperature at the outer component surface is equal to the measured values or changes according to the prescribed time function, is a very difficult task.

Many numerical, analytical, and semi-analytical [14] approaches have been developed for solving IHCPs. Explicit analytical solutions are limited to simple geometries, but are very efficient computationally and are of fundamental importance for investigating basic properties of IHCPs.

The problem of optimum heating or cooling will be solved under the assumption that physical properties of the component material and the heat transfer coefficient are constant.

The aim of the paper is to show how difficult the inverse heat conduction problem (IHCP) is. Even for the simple IHCP, when the temperature changes are exactly known at the interior point, it is impossible to find a unique solution at the initial stage of the transient process. The discussion focuses on sequential inverse methods, which are widely used in on-line thermal stress monitoring systems. Whole domain estimation procedures, based on simultaneously determining all the unknown parameters for the total time interval, are less appropriate for on-line applications, since the entire time history of the measured temperature is not known in advance. Data points are only available over the time interval from initial time till the moment under consideration. In addition, the time of computation should be smaller than the data sampling period.

A new procedure for the solution of the linear IHCP based on a numerical approximation of Duhamel's integral in conjuction with future time steps is presented.

This method and four other techniques: the Laplace Transform method, the modified Burggraf solution, the space marching method, and the whole domain least squares method will be used for solving optimum heating problem when linear time temperature variation is prescribed at the insulated rear surface of the plate. New solutions for the fluid temperature changes for this specific problem will be found.

Moreover, the optimum fluid temperature changes obtained by the various methods considered in the paper will be compared.

It must be emphasized that all the methods analyzed in the paper exhibit some problems in determining initial optimum fluid temperature changes if the wall temperature changes are prescribed at the rear insulated surface. The optimum fluid temperature changes, obtained by various methods, differ significantly. The problems encountered in the methods used in the paper will be discussed in detail.

2. Mathematical formulation of the problem

In the case of time-dependent boundary conditions, the solution for the linear initial-boundary problem can be significantly simplified by applying Duhamel's integral

$$S\left(\mathbf{r}_p,t\right)=$$

$$S_0 + \int_0^t \left[T_f\left(\Theta\right) - T_0 \right]\frac{\partial u\left(\mathbf{r}_P,t-\Theta\right)}{\partial t}d\Theta = S_0 + \int_0^t \frac{d\left[T_f\left(\Theta\right) - T_0 \right]}{d\Theta}u\left(\mathbf{r}_P,t-\Theta\right)d\Theta \tag{1}$$

where $S\left(\mathbf{r}_P,t\right)$ is the solution of the initial-boundary problem with time-dependent fluid temperature $T_f\left(t\right)$ at the location $\mathbf{r}_p$ and time t.

The initial value S_0 is a constant and does not depend on the location. Function $u\left(\mathbf{r}_P, t\right)$ is the solution for the initial-boundary problem with unit step increase of the fluid temperature $T_f\left(t\right) = 1, \; t > 0$. When the solution $u\left(\mathbf{r}_P, t\right)$ for the unit fluid temperature change described by the Heaviside function is known, it is easy to determine the solution $S\left(\mathbf{r}, t\right)$ or the time-dependent fluid temperature $T_f\left(t\right)$. In optimization of heating or cooling of the construction element, the desired system response $y\left(t\right) = S\left(\mathbf{r}_P, t\right)$ at the inner point $\mathbf{r}_P$ is given and the time changes of the fluid temperature $T_f\left(t\right)$

$$\int_0^t \left[T_f\left(\Theta\right) - T_0\right] \frac{\partial u\left(\mathbf{r}_P, t - \Theta\right)}{\partial t} d\Theta = y\left(t\right) - S_0 \qquad (2)$$

is searched for.

The optimization problem is reduced to the solution of the Volterra integral equation of the first kind.

To evaluate the convolution integral in equation (2), the real changes of the function $f(\Theta) = T_f(\Theta) - T_0$ are replaced by a step-wise function

$$
\begin{aligned}
f_1 &= f\left(\Theta_1 / 2\right), & 0 \le \Theta \le \Theta_1 \\
f_2 &= f\left[\Theta_1 + \left(\Theta_2 - \Theta_1\right)/2\right] & \Theta_1 \le \Theta \le \Theta_2 \\
&\vdots \\
f_M &= f\left[\Theta_{M-1} + \left(\Theta_M - \Theta_{M-1}\right)/2\right] & \Theta_{M-1} \le \Theta \le \Theta_M
\end{aligned}
\qquad (3)
$$

where M is the number of time steps.

A simple way of determining the integral in equation (2) is the method of rectangles. However, in case of too small integration time steps $\Delta\Theta_i = \Theta_i - \Theta_{i-1}$ unexpected instabilities can appear in the estimated function $f\left(t\right)$.

To assure the stability of the calculations, the time step Δt of determining the fluid temperature $T_f\left(t\right)$ should be larger than the critical value Δt_{cr} evaluated from the condition

$$\Delta t_{cr} = \frac{\Delta Fo_{cr}\; d^2}{\alpha} \tag{4}$$

where $\Delta Fo_{cr} \cong 0.5$ and $d = \min\left|\mathbf{r}_P - \mathbf{r}_S\right|$ is the distance between the point P and the body surface and denotes the thermal diffusivity of the body.

In practice, time step Δt given by equation (4) is too big, making it impossible to reconstruct the rapidly changing fluid temperature $T_f \left(t \right)$ that causes a specified output $y(t)$ inside the body or on its surface.

This problem is especially important at the beginning of the optimum heating or cooling process. In this paper, so-called future time steps are used for stabilising the solution of the inverse problem. These were introduced by Beck in the inverse problem analysis. The efficiency of the future time steps results from the artificial extension of the basic time step Δt. This approach is very useful in inverse problems because the time changes of the fluid temperature $T_f \left(t \right)$ received in the interior point $\mathbf{r}_p$ are significantly delayed and damped.

Evaluation of $f_i, \ i = 1, ..., M$ will be performed step by step. First, f_1 will be evaluated, then f_2, etc. In each case it is assumed that the values of $S \ \mathbf{r}_P, t_{M-1}$ and f_{M-1} are known. The f_M value remains to be calculated in the time interval $t_{M-1} \le t \le t_M$ (Fig. 1). The time interval will be artificially extended by F future time steps, with the assumption, that in the extended interval, the $t_{M-1} \le t \le t_{M+F}$ value of the function $f \ t$ remains constant and equals f_M, i. e.,

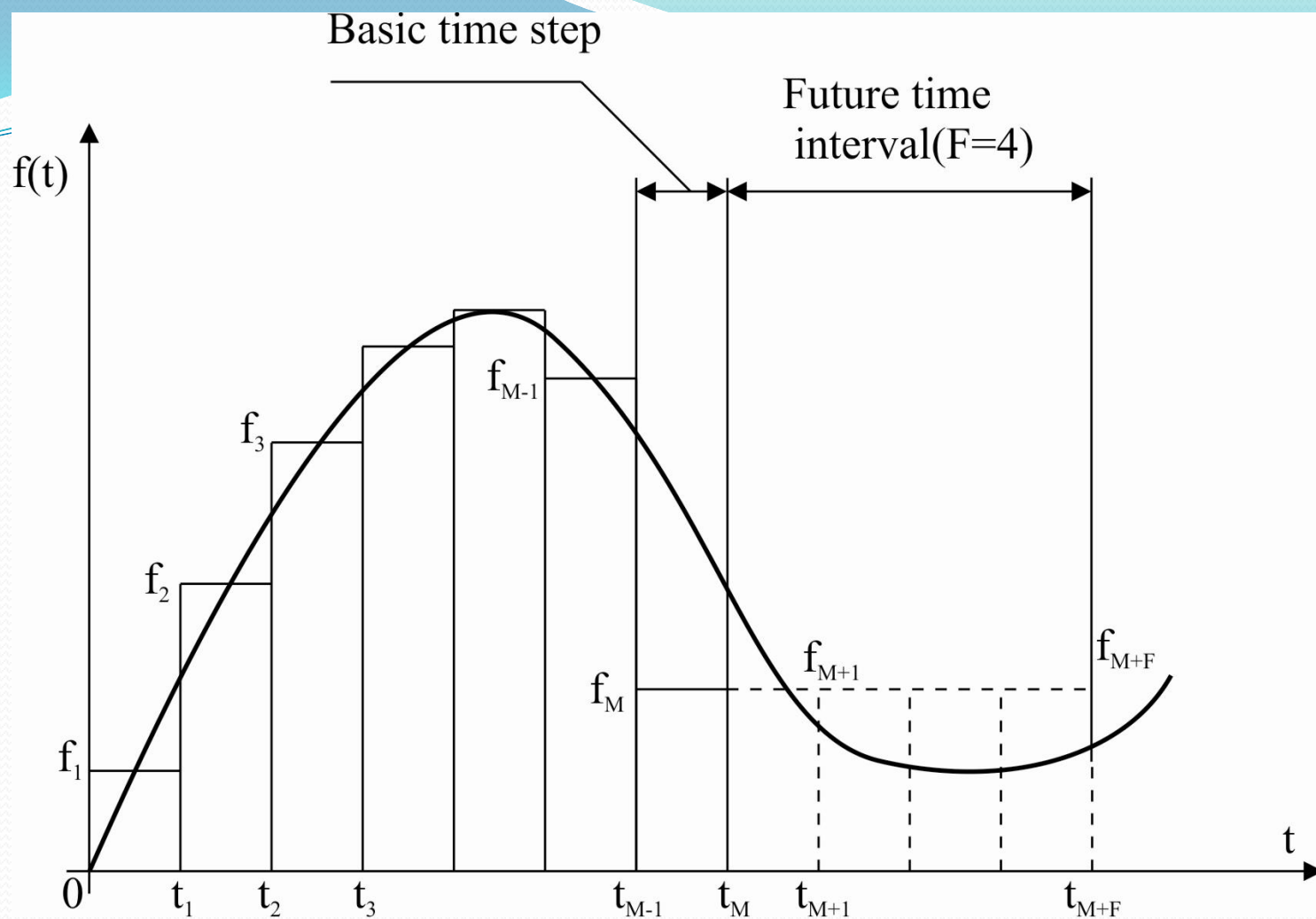$$f_{M+1} = f_{M+2} = \ldots = f_{M+F} = f_M \qquad (5)$$

Fig.1. Stepwise approximation for $f\left(t\right) = T_f\left(t\right) - T_0$ and use of future temperatures to stabilise the inverse problem of optimum heating

The value of the fluid temperature (input signal) $f_M = T_f \left(t_M \right)$ is determined from the equation (2) which can be written in the form:

$$S \left(\mathbf{r}_P, t_{M+F} \right) - y \left(t_{M+F} \right) = 0 \qquad\qquad (6)$$

It is assumed that the value f_M evaluated in this way is valid only in the interval $t_{M-1} \le t \le t_M$.

The convolution integral in equation (1) can be calculated numerically using the method of rectangles

$$S\left(\mathbf{r}_P, t_{M+F}\right) = S_0 + \int_0^{t_{M+F}} f(\Theta) \frac{\partial u\left(\mathbf{r}_P, t - \Theta\right)}{\partial \Theta} d\Theta \cong$$

$$S_0 + f_1 \Delta u_{M+F} + f_2 \Delta u_{M+F-1} + \ldots + f_{M+F} u_1 =$$

$$S_0 + \sum_{i=1}^{M-1} f_i \Delta u_{M+F-i} + \left(\Delta u_F + \Delta u_{F-1} + \ldots + u_1\right) f_M =$$

$$S_o + \sum_{i=1}^{M-1} f_i \Delta u_{M+F-i} + u_{F+1} f_M ,$$

(7)

where

$$\Delta u_0 = u_1 - u_0 = u_1, \quad \Delta u_i = u_{i+1} - u_i, \quad u_n = \sum_{i=0}^{n-1} \Delta u_i .$$

(8)

Substituting (7) into (6) yields

$$f_1 = \frac{y\ t_{F+1} - S_0}{u_{F+1}} \qquad (9)$$

and

$$f_M = \frac{y\ t_{M+F} - S_0 - \sum_{i=1}^{M-1} f_i\ \Delta u_{M+F-i}}{u_{F+1}}, \qquad M = 2,3,\dots \qquad (10)$$

Equations (9) and (10) allow us to sequentially calculate $f_1,\ f_2, f_3,$ etc. The time interval $\Delta t_M = t_M - t_{M-1}$ does not have to be as large as given by equation (4). If $F \geq 1$, the time step Δt can be several times smaller. Stable solutions are already obtained at $\Delta Fo_{cr} \cong 0.05$. In comparison with $\Delta Fo_{cr} \cong 0.5,\ \Delta Fo_{cr} \cong 0.05$ denotes a significant increase in the frequency of determining $f_i,\ i = 1, 2, 3, ...$. Future time steps increase the stability of the calculations, however they diminish the accuracy of $f\ t$ estimation.

The Laplace Transform is another method that allows determining optimum fluid temperature changes. By taking the Laplace Transforms of both sides of the equation (2) we obtain

$$\left[\bar{T}_f\left(s\right) - \frac{T_0}{s} \right]\left[s\bar{u}\left(\mathbf{r}_P, s\right) - u\left(\mathbf{r}_P, 0\right) \right] = \bar{y}\left(s\right) - \frac{S_0}{s} \qquad (11)$$

which can be solved for $\bar{T}_f\left(s\right)$, so that

$$\bar{T}_f\left(s\right) = \frac{T_0}{s} + \frac{\bar{y}\left(s\right) - \dfrac{S_0}{s}}{s\bar{u}\left(\mathbf{r}_P, s\right) - u\left(\mathbf{r}_P, 0\right)} \qquad (12)$$

Where s is the complex variable.

The initial value of $u\left(\mathbf{r}_P, t\right)$ is $u\left(\mathbf{r}_P, 0\right) = 0$. In order to find the corresponding function of time $T_f\left(t\right)$, an inversion of the Laplace Transform (12) can be performed analytically or numerically. In the numerical procedures for finding the inverse Laplace Transforms, the time sampling interval Δt must be sufficiently large enough to obtain stable results for $T_f\left(t\right)$. This is the main drawback of using the Laplace Transform based method to determine the optimum changes of $T_f\left(t\right)$. If the point $\mathbf{r}_p$ is situated at a large distance from the heated surface, then the time interval Δt should be large enough to assure the stability of the solution. The requirement of large time steps does not allow determining quick changes of the fluid temperature $T_f\left(t\right)$, which occur at the initial period of optimum heating.

The third method, which can be used to determine the optimum fluid temperature $T_f(t)$, is the analytical solution of the inverse heat conduction problem presented by Burggraf. The Burggraf method is appropriate only for one-dimensional problems and does not allow us to determine the optimum temperature $T_f(t)$ at the initial time period.

The same drawback has the solution obtained by the space marching method, which is identical to that obtained by the Burggraf method.

In the fifth method a time function representing optimum changes of the fluid temperature is assumed and unknown parameters are estimated using the least squares method.

3. Example of applications

      The objective of this example is to determine the optimum temperature changes $T_f\ t$ for which the temperature of the slab in the point increases linearly with time

$$S\ \mathbf{r}_{\mathrm{P}},t\ =T\ x_T,t\ =v_T\,t \tag{13}$$

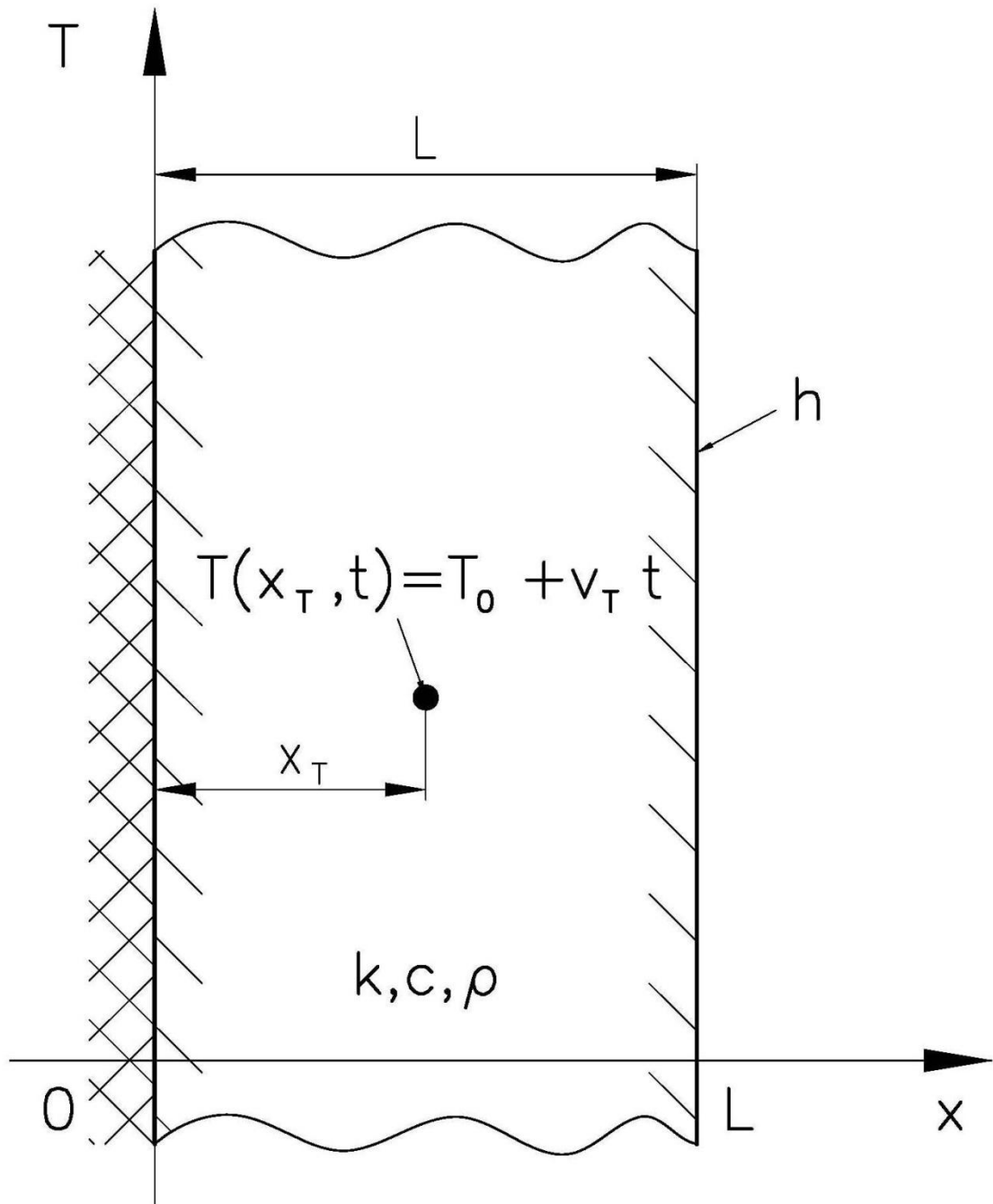where v_T is the constant temperature rate (Fig.2).

Fig.2. Location x_T, at which temperature changes according to the prescribed function $T\left(x_T,t\right) = T_0 + v_T\, t$.

The mathematical formulation of the problem is

$$c\,\rho\frac{\partial T}{\partial t} = k\frac{\partial^2 T}{\partial x^2}, \quad t > 0 \qquad (14)$$

$$T\left(x,0\right) = T_0, \quad 0 \le x \le L \qquad (15)$$

$$\frac{\partial T}{\partial x}\bigg|_{x=0} = 0, \quad t > 0 \qquad (16)$$

$$T\left(x_T,t\right) = y\left(t\right) = T_0 + v_T \cdot t, \quad 0 \le x_T \le L, \quad t > 0 \qquad (17)$$

$$k\frac{\partial T}{\partial x}\bigg|_{x=L} = h\left[T_f\left(t\right) - T\big|_{x=L}\right], \quad t > 0 \qquad (18)$$

The boundary condition of the third kind is given at the exposed surface. The time varying fluid temperature $T_f\ t$ will be determined from the solution of the problem (14-18).

Calculations were carried out for the slab of thickness $L = 0.1$ m with the uniform initial temperature $T_0 = 0^o C$. The physical properties of the slab made from carbon steel are: ρ=7800 kg/m³, c=482 J/(kgK), k=42 W/(mK), where ρ - density, c - specific heat capacity and k - thermal conductivity. The heat transfer coefficient at the exposed slab surface is h=2000 W/m² K. The rear surface of the slab is thermally insulated. The temperature of the rear surface (x_T = 0) increases with the constant rate $v_T = 0.1K/s$. The methods described above will be used for determining $T_f\ t$.

3.1. Approximate solution based on the numerical integration of the convolution integral

In order to calculate f_i, $i = 1, \ldots, M$ by using formulas (9-10) it is necessary to solve the heat conduction equation (14) with the conditions (15), (16) and (18) for $T_f = 1°C$, $t > 0$. The exact analytical solution of this problem is:

$$u\left(x,t\right) = 1 - \sum_{n=1}^{\infty} \frac{2\sin\mu_n}{\mu_n + \sin\mu_n \cos\mu_n} \cos\left(\mu_n \frac{x}{L}\right) \exp\left(-\mu_n^2 \frac{\alpha t}{L^2}\right) \qquad (19)$$

where: $\alpha = k / c\rho$ is thermal diffusivity, μ_n are the positive roots of $\mu_n \operatorname{tg}\mu_n = Bi$, and $Bi = hL / k$ is the Biot number.

Optimum fluid temperature changes are shown in Fig. 7. Since the point P is located on the rear, insulated surface not directly adjacent to the fluid, the future time steps were used (F=5). The phenomenon of strong damping and delaying of temperature changes $T_f\left(t\right)$ at the body inside causes large discrepancies in the estimated changes of $T_f\left(t\right)$ for small time values. After the initial allowable temperature increase over 200°C, a rapid decrease in temperature T_f to about 80°C occurs, and then the temperature rises with a constant rate of $v_T = 0.1\text{K}/\text{s}$.
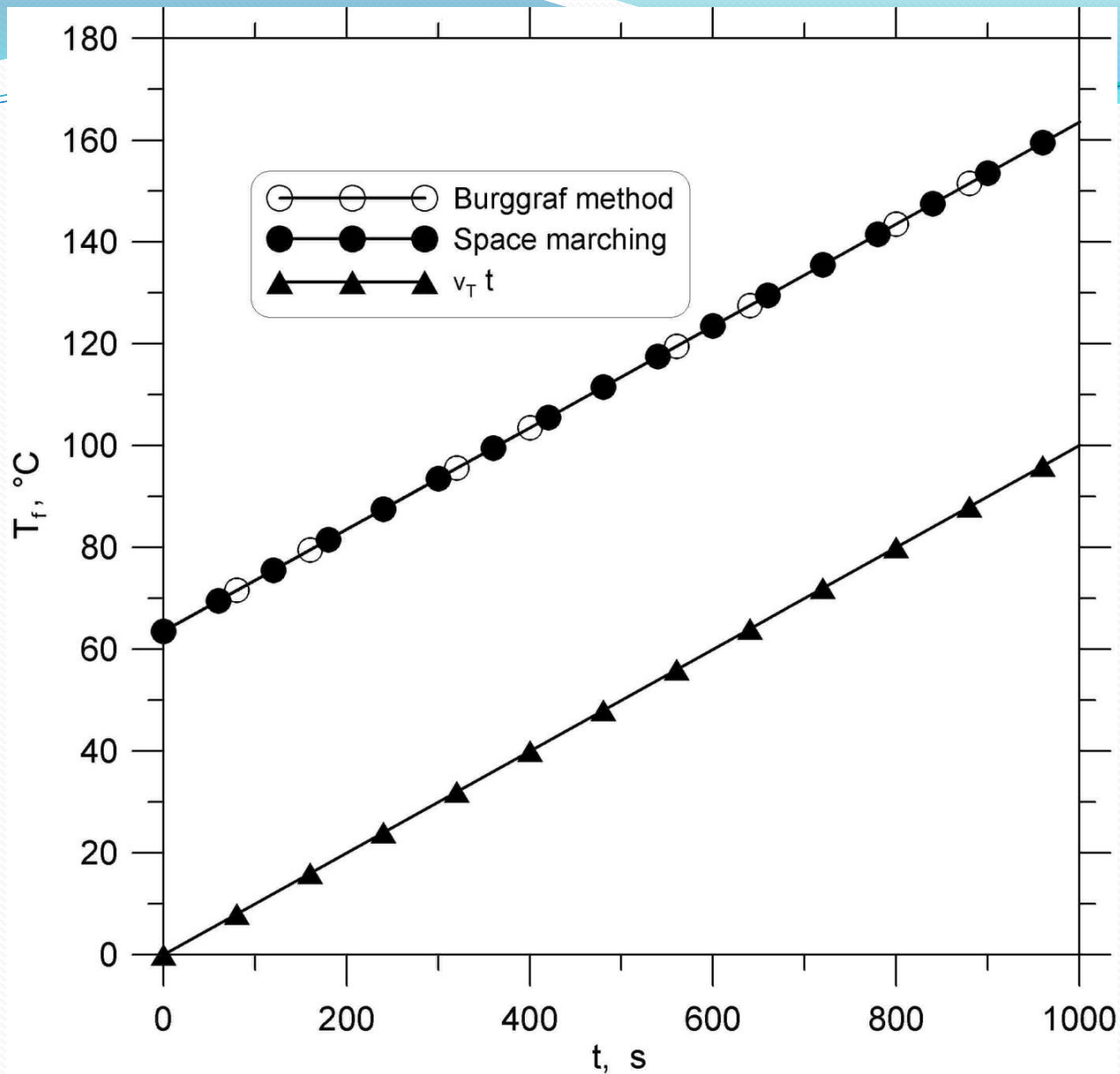
Fig.3. Optimum fluid temperature changes obtained by using the Burggraf solution and space marching method

3.2. Determination of the optimum fluid temperature changes using the Laplace Transform

If the prescribed temperature changes of the slab at location x_T are given by the equation (13), then the Laplace Transform (12) becomes

$$\bar{T}_f\left(s\right) = \frac{T_0}{s} + \frac{v_T}{s^2}\frac{\dfrac{k}{h}q\sinh\left(qL\right) + \cosh\left(qL\right)}{s^2\cosh\left(q\,x_T\right)}\ , \qquad (20)$$

where: $q = \sqrt{s/\alpha}$.

Applying the inverse Laplace Transforms to the equation (20) gives

$$T_f\ t\ = T_0 + v_T \left\{ t + \frac{L^2}{\alpha} \left[\frac{1}{Bi} + \frac{1}{2}\left(1 - \frac{x_T^2}{L^2} \right) \right] \right\} +$$

$$+ \frac{2x_T^2 v_T}{\alpha} \sum_{n=1}^{\infty} \frac{cos\left(\frac{2n-1}{2}\pi\frac{L}{x_T} \right) - \frac{1}{Bi}\left(\frac{L}{x_T} \right)\left(\frac{2n-1}{2}\pi \right) sin\left(\frac{2n-1}{2}\pi\frac{L}{x_T} \right)}{-1^{\ n-1}\left(\frac{2n-1}{2}\pi \right)^3} \times \qquad (21)$$

$$\times exp\left[-\frac{\alpha t}{x_T^2}\left(\frac{2n-1}{2}\pi \right)^2 \right]$$

where: $\quad Bi = hL / k$.

The expression (21) represents the exact solution of the problem (14-18). In practice, it is difficult to find temperature $T_f\ t$ for $0 \le\ x_T\ /L \le 1$, because the exponential term in (21) is close to zero and the equation (21) reduces to the quasi-steady-state solution

$$T_f\ t\ = T_0 + v_T \left\{ t + \frac{L^2}{\alpha} \left[\frac{1}{Bi} + \frac{1}{2} \left(1 - \frac{x_T^2}{L^2} \right) \right] \right\}$$ (22)

Thus, the form of the equation (21) is not appropriate for determining optimum temperature changes of the fluid in the early time stages of the slab heating, if $x_T\ /L \le 1$.

3.3. Determination of the optimum fluid temperature changes by using the Burggraf and space marching methods

Burggraf presented one of the earliest analytical solutions of the one-dimensional inverse heat conduction problem. When $x_T = 0$, then applying the Burggraf method to the inverse problem yields

$$T_B \left(x,t \right) = y(t) + \sum_{n=1}^{\infty} \frac{1}{2n\,!} \frac{x^{2n}}{\alpha^n} \frac{d^n y}{dt^n} = T_0 + v_T t + v_T \frac{x^2}{2\alpha} \qquad (23)$$

Inserting equation (23) in (18) and solving for $T_f \left(t \right)$ gives

$$T_f \left(t \right) = T_0 + v_T \left[t + \frac{L^2}{\alpha} \left(\frac{1}{Bi} + \frac{1}{2} \right) \right] \qquad (24)$$

Thus, the obtained result (24) is identical with the quasi-steady-state solution (22) and is not adequate for small time values. It is worth mentioning that the same solution (24) gives the space marching method.

Examining the function (23) at $t = 0$ shows, that the initial temperature distribution is non-uniform

$$T_B\left(x, 0\right) = T_0 + \frac{v_T x^2}{2\alpha} \tag{25}$$

In order to alleviate this difficulty the general problem given by equations (14-17) may be separated in accordance with the superposition method into a set of simpler problems containing: a homogenous transient problem and quasi-steady-state problem.

The optimum fluid temperature changes T_f t , which were calculated using Eq. (24) and the space marching method developed in [14], are shown in Fig. 3. Taking into account that that the temperatures at the boundaries are: $T_B(0, t) = v_T t$ and $T_B(L, t) = v_T [t + L^2/(2\alpha)]$, the method of superposition will be used to satisfy the initial condition given by Eq.(15). The transient temperature distribution T_T is the solution of the heat conduction equation

$$c\,\rho\frac{\partial T_T}{\partial t} = k\frac{\partial^2 T_T}{\partial x^2}, \quad t > 0 \tag{26}$$

with the boundary conditions

$$T_T \big|_{x=0} = 0 \qquad\qquad (27)$$

$$T_T \big|_{x=L} = 0 \qquad\qquad (28)$$

and the initial condition

$$T_T \big|_{t=0} = -\frac{v_T x^2}{2\alpha} \qquad\qquad (29)$$

Solving the initial-boundary value problem defined by Eqs (26)-(29) using the method of variable separation yields the transient temperature distribution $T_\text{T}(x,t)$. The complete solution for temperature distribution $T = T_B + T_T$, that satisfies the initial condition (15), can be expressed as

$$T\ x,t\ = T_0 + v_T\left(t + \frac{x^2}{2\alpha}\right) + $$

$$+ \frac{v_T L^2}{\alpha}\sum_{n=1}^{\infty}\frac{1}{n\pi}\left[\ -1\ ^n\left(1 - \frac{2}{n^2\pi^2}\right) + \frac{2}{n^2\pi^2}\right]\sin\left(n\pi\frac{x}{L}\right)\exp\left(-n^2\pi^2\frac{\alpha t}{L^2}\right).$$

(30)

The transient part T_T of the complete solution T which is needed to improve the quasi-steady-state solution (Burggraf solution) is shown in Fig. 4.
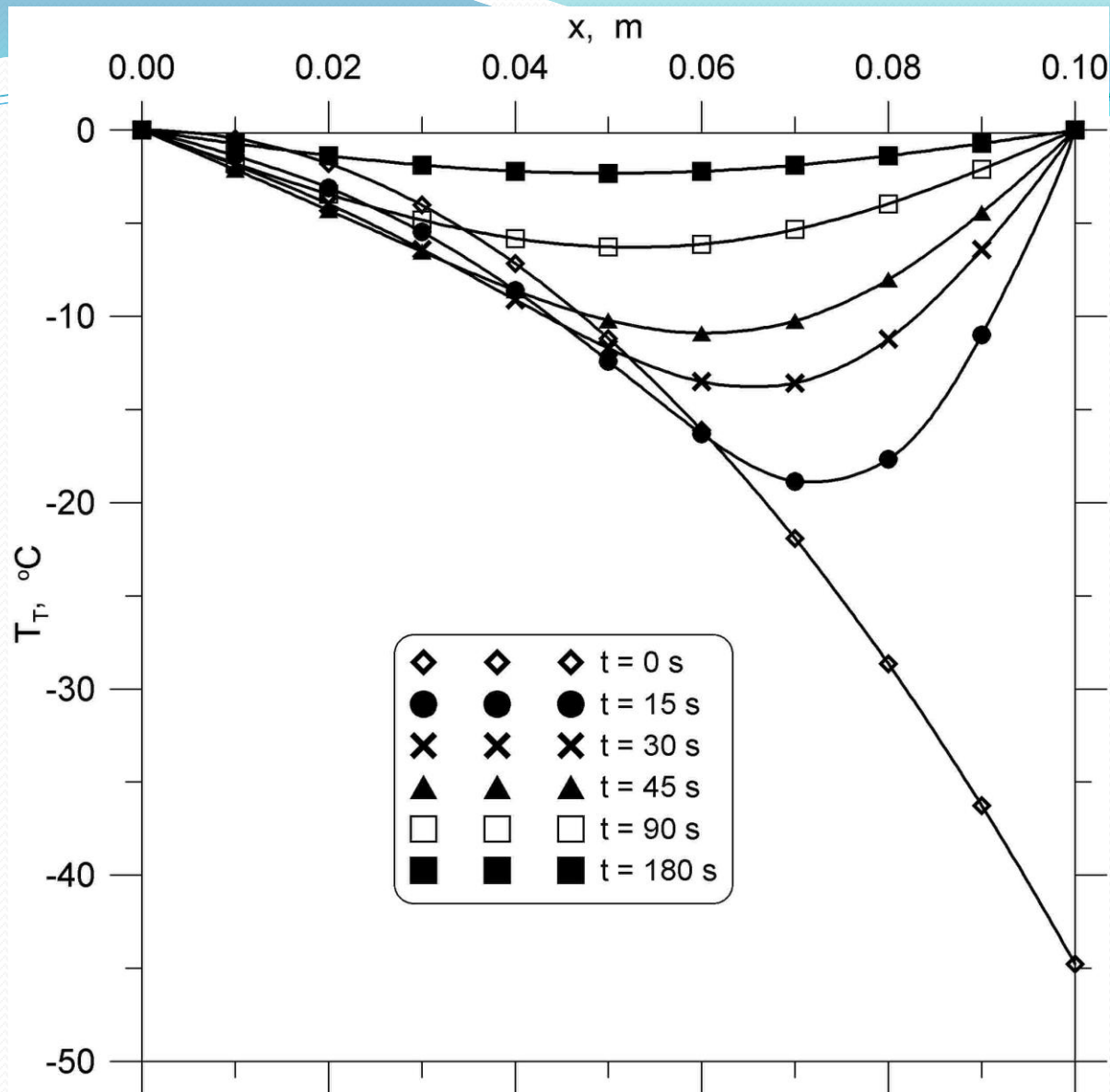
Fig.4. Transient part of temperature distribution which is needed for modifying the Burggraf solution

The heat flux $\dot{q}\left(x,t\right)$ is given by

$$\dot{q}\left(x,t\right) = k\frac{\partial T}{\partial x} = c\rho v_T x +$$

$$+c\rho v_T L\sum_{n=1}^{\infty}\left[\left(-1\right)^n\left(1-\frac{2}{n^2\pi^2}\right)+\frac{2}{n^2\pi^2}\right]\cos\left(n\pi\frac{x}{L}\right)\exp\left(-n^2\pi^2\frac{\alpha t}{L^2}\right).$$

(31)

The optimum heat flux at the exposed surface is shown in Fig. 5.
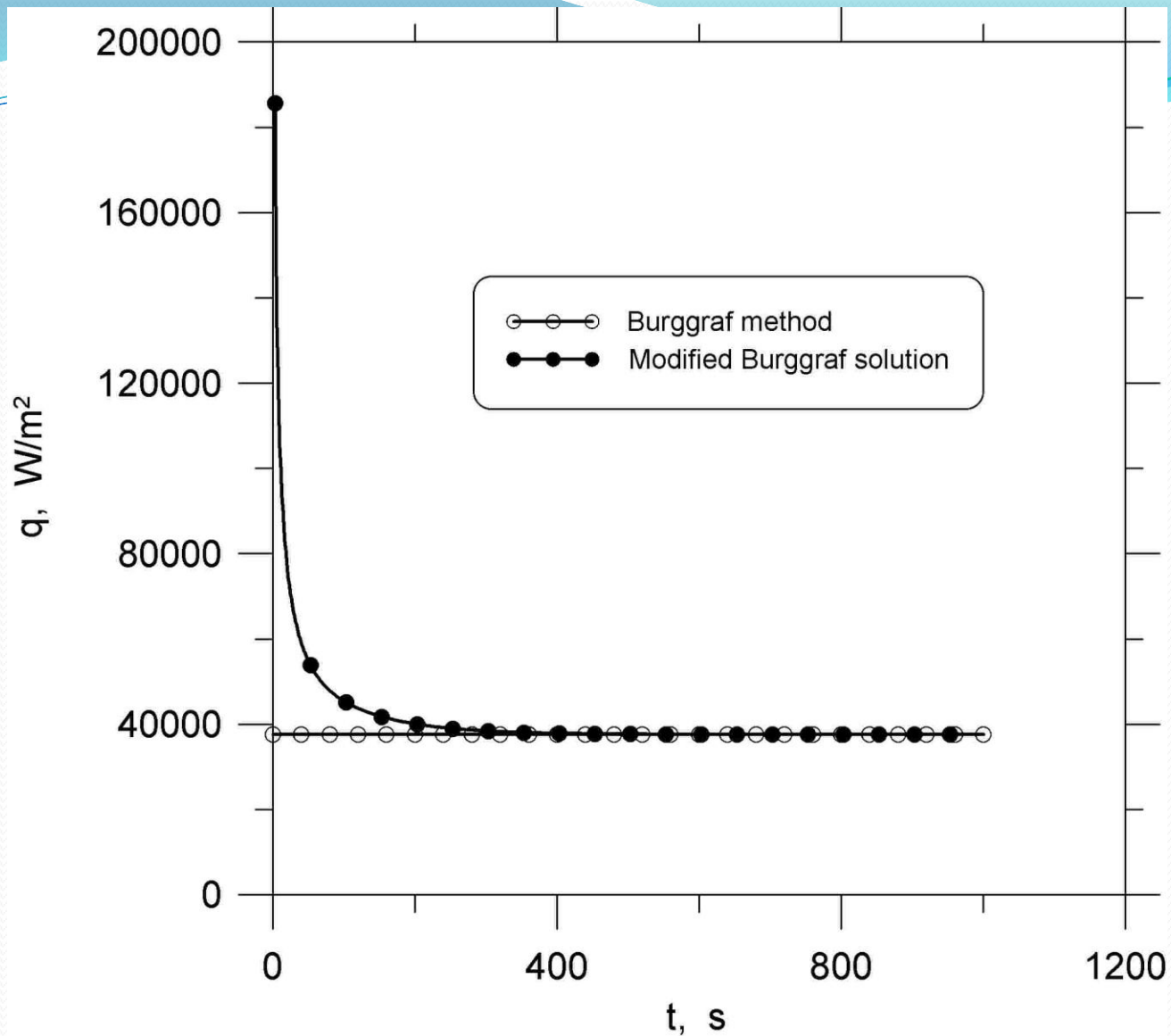
Fig.5. Heat flux at the exposed surface during optimum heating

The optimum fluid temperature $T_f\left(t\right)$ is determined from equation (18) as

$$T_f\left(t\right) = T\big|_{x=L} + \frac{k}{h}\frac{\partial T}{\partial x}\bigg|_{x=L} \qquad (32)$$

Where $T\left(x,t\right)$ and $k\partial T/\partial x$ are defined by equations (30) and (31), respectively. The optimum temperature history $T_f\left(t\right)$ calculated according to equation (30) is compared in Fig.3 with the approximate solution based on the numerical integration of the convolution integral. The deviations between the estimated and optimum temperatures $T_f\left(t\right)$ were found to decrease with increasing time intervals. The temperature distribution across the slab thickness during the optimum heating is shown in Fig.6.
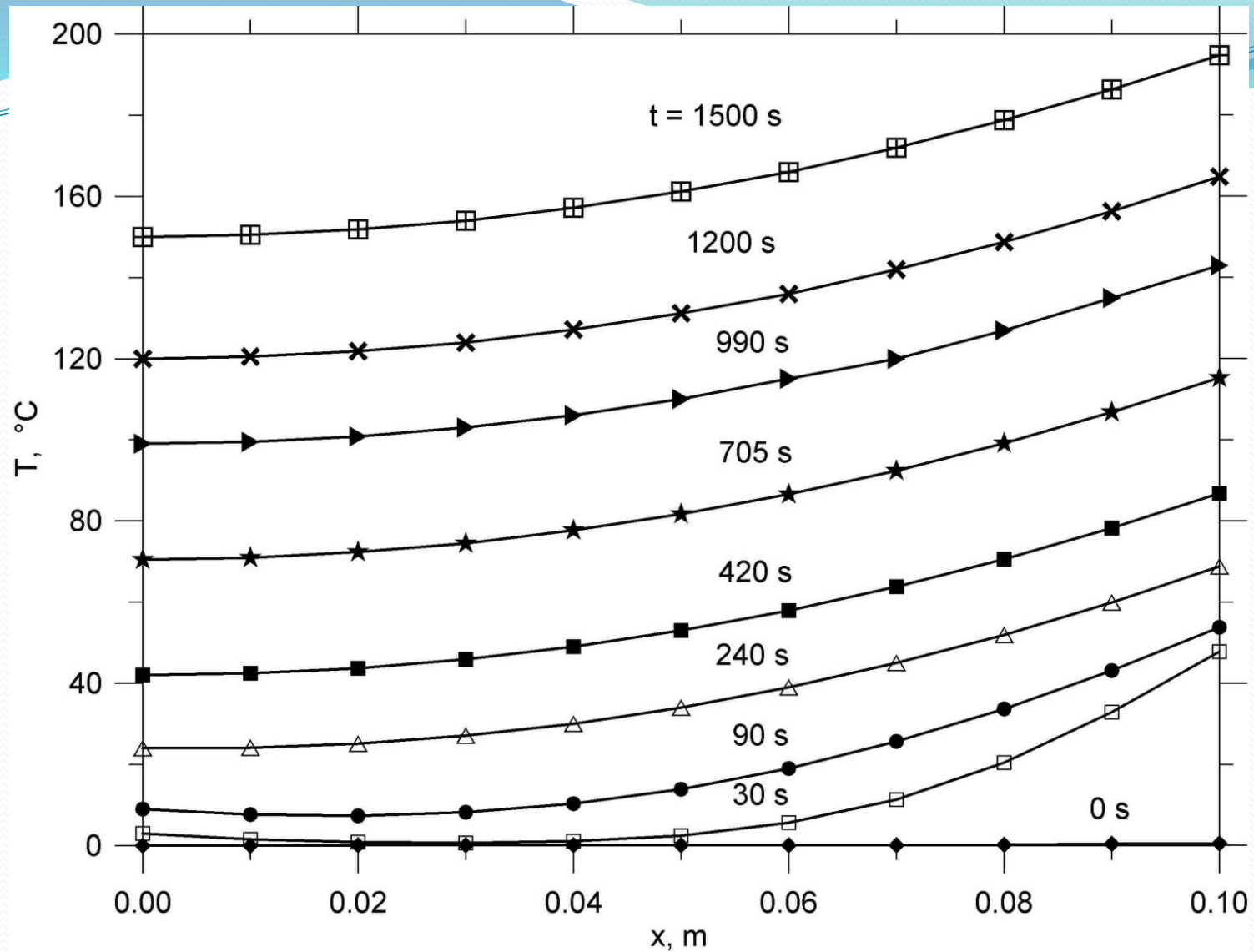
Fig.6. Transient temperature distribution in a slab during optimum heating

3.4. Determination of the optimum fluid temperature changes by solving the parametric least squares problem

Optimum changes of the fluid temperature T_f during heating of the slab, which are shown in Fig. 7, are very difficult to carry out in practice for the initial stage of the component heating. However, optimum fluid temperature changes can be approximated by a ramp function consisting of a step increase in fluid temperature T_s followed by the temperature increase with a constant rate v_T.
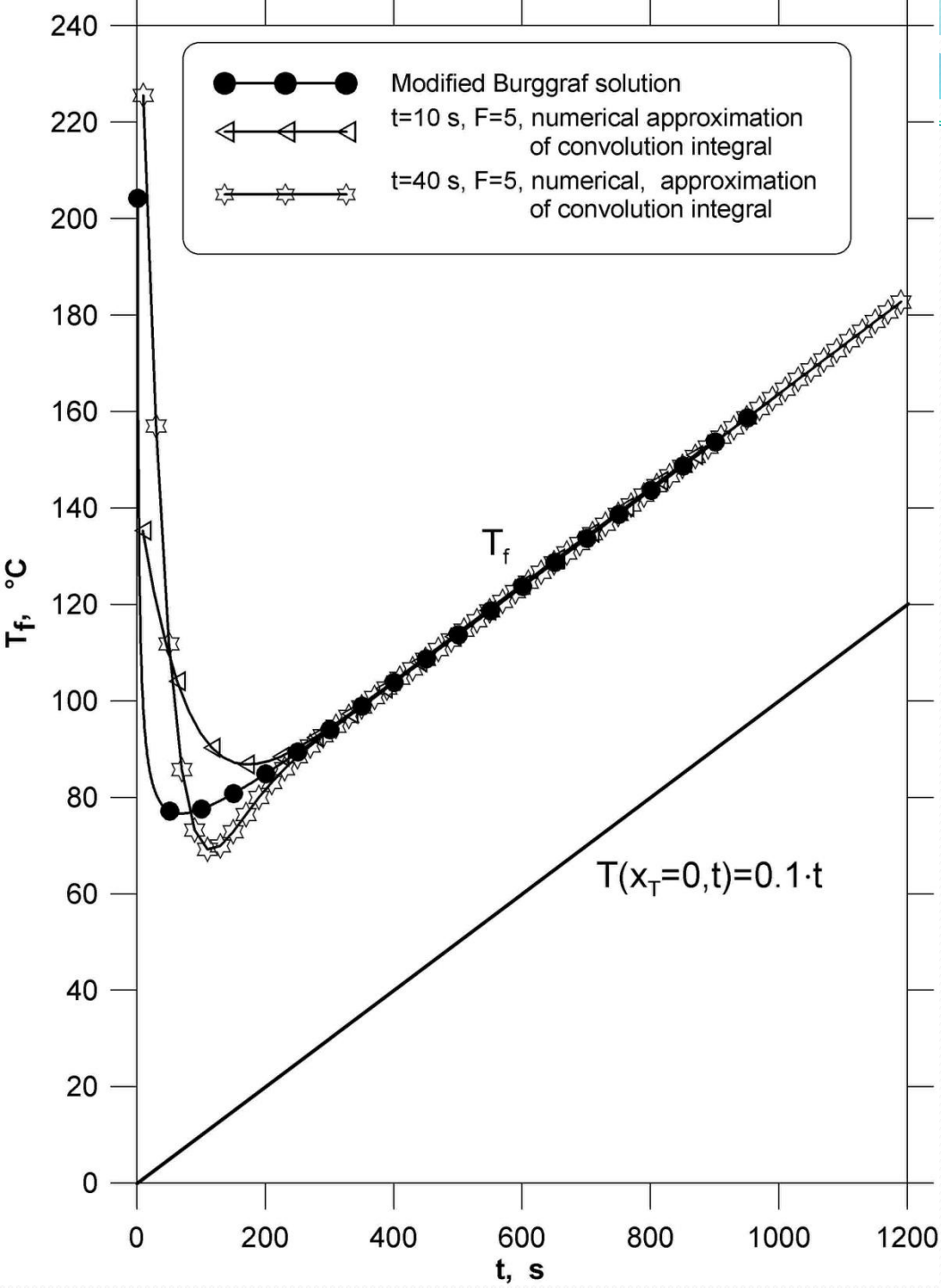
Fig.7. Optimum changes of the fluid temperature T_f during heating of the slab with the prescribed temperature of the insulated rear side:

$$T\left(0,t\right) = 0.1 \cdot t.$$

The solution of the direct heat conduction problem, which is defined by the heat conduction equation (14), initial condition (15), boundary conditions (16) and (18) with the fluid temperature given by

$$T_f\left(t\right) = T_0 + T_s + v_T t \tag{33}$$

is as follows

$$T\left(x,t\right) = T_0 + \int_0^t \frac{d\left[T_f\left(\theta\right) - T_0\right]}{dt} u\left(x,t-\theta\right) d\theta \tag{34}$$

where the influence function $u(x,t)$ is defined by Eq.(19).

Substituting Eqs (19) and (33) into Eq. (34) and integrating gives

$$T\left(x,t\right) = T_s + \left(T_0 - T_s\right) F_1\left(x,t\right) + v_T t - v_T F_2\left(x,t\right) \tag{35}$$

where

$$F_1\left(x,t\right) = \sum_{n=1}^{\infty} \frac{2\sin\mu_n}{\mu_n + \sin\mu_n \cos\mu_n} \cos\left(\mu_n \frac{x}{L}\right) \exp\left(-\mu_n^2 \frac{\alpha t}{L^2}\right) \tag{36}$$

$$F_2\left(x,t\right) = \frac{L^2}{\alpha}\left[\frac{1}{Bi} + \left(1 - \frac{x}{L}\right) - \frac{1}{2}\left(1 - \frac{x}{L}\right)^2 - \right.$$

$$\left. -\sum_{n=1}^{\infty} \frac{2\sin\mu_n}{\mu_n^2\left(\mu_n + \sin\mu_n \cos\mu_n\right)} \cos\left(\mu_n \frac{x}{L}\right) \exp\left(-\mu_n^2 \frac{\alpha t}{L^2}\right)\right] \tag{37}$$

In the inverse problem, the unknown parameters T_s and v_T are to be adjust to satisfy approximately the following system of equations

$$y\left(t_i\right) - T\left(x_T, t_i\right) \cong 0, \ i = 1,\ldots,n_t. \tag{38}$$

where the prescribed temperature $y(t)$ changes at the location x_T are given by Eq. (17).

The least squares method is used to estimate parameters T_s and v_T. The parameters T_s and v_T are computed by minimizing the sum of squares of the differences between values given by the model (39) and those obtained from Eq. (17):

$$S_L = \sum_{i=1}^{n_t}\left[y\left(t_i\right) - T\left(x_T, t_i\right)\right]^2. \tag{39}$$

It is necessary to find the values of T_s and v_T, for which the two partial derivatives are simultaneously zero:

$$\frac{\partial S_L}{\partial T_s} = 0, \qquad \frac{\partial S_L}{\partial v_T} = 0. \qquad (40)$$

Finding dervatives (40) gives a set of linear equations in the unknowns T_s and v_T, which has the following solution

$$T_s = \frac{b_1 a_{22} - b_2 a_{12}}{a_{11} a_{22} - a_{21} a_{12}} \qquad (41)$$

$$v_T = \frac{b_2 a_{11} - b_1 a_{21}}{a_{11} a_{22} - a_{21} a_{12}} \qquad (42)$$

where

$$a_{11} = \sum_{i=1}^{n_t} \left[1 - F_1\left(x_T, t_i\right) \right]^2, \quad a_{12} = \sum_{i=1}^{n_t} \left[1 - F_1\left(x_T, t_i\right) \right] \left[t_i - F_2\left(x_T, t_i\right) \right],$$

$$a_{21} = a_{12}, \quad a_{22} = \sum_{i=1}^{n_t} \left[t_i - F_2\left(x_T, t_i\right) \right]^2,$$

$$b_1 = -\sum_{i=1}^{n_t} \left[1 - F_1\left(x_T, t_i\right) \right] \left[T_0 F_1\left(x_T, t_i\right) - y_i \right],$$

$$b_2 = -\sum_{i=1}^{n_t} \left[t_i - F_2\left(x_T, t_i\right) \right] \left[T_0 F_1\left(x_T, t_i\right) - y_i \right].$$

(43)

The discrepancy between the prescribed function $y(t)$ and the fitting function $T(x_T,t)$ can be quantified by the mean square error (standard deviation), defined as

$$\sigma = \sqrt{\frac{S_L}{n_t - m}} \qquad (44)$$

The symbol m denotes the number of parameters to be estimated. In this example, m is 2. The values of T_s and v_T are also determined by the modified Levenberg-Marquardt method using the subroutine BCLSF from the IMSL mathematical library.

As an example, we shall fit the solution (35) to the function $y = 0.1t$.

As the time points t_i are equally distributed with the time step Δt, the time points t_i are given by

$$t_i = i\Delta t, \quad i = 1, \ldots, n_t \tag{45}$$

The number of time points n_t is 100. Parameters T_s and v_T were computed for three different time steps Δt : 12 s, 30 s, and 60 s. The following results were obtained:

- $T_s = 81.2176\,^oC, \ v_T = 0.07308\,K\,/\,s, \ S_L = 984.73\,K^2, \ \sigma = 3.17\ K\ for\ \Delta t = 12\ s,$
- $T_s = 68.8978\,^oC, \ v_T = 0.09700\,K\,/\,s, \ S_L = 706.43\,K^2, \sigma = 2.68\ K\ for\ \Delta t = 30\ s,$
- $T_s = 65.8331\,^oC, \ v_T = 0.09939\,K\,/\,s, \ S_L = 440.35\,K^2, \sigma = 2.12\ K\ for\ \Delta t = 60\ s.$

The same results were obtained using the Levenberg-Marquardt method.
The computed fluid and wall temperatures are shown in Figs. 8a, 8b, and 8c.
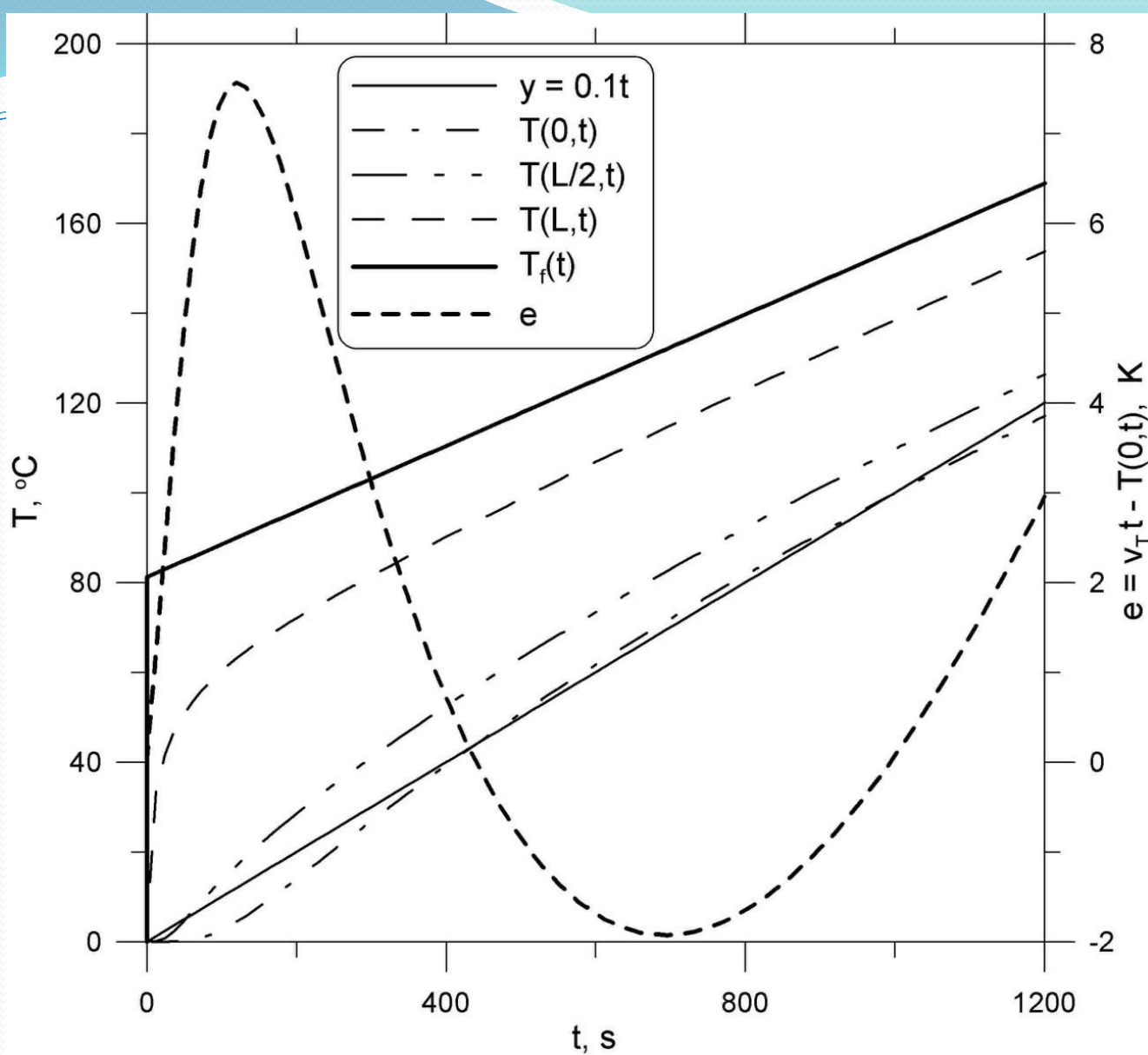
Fig.8a. Fluid and slab temperature changes when optimum fluid temperature changes are approximated by a ramp function; $\Delta t = 12\text{s}$.
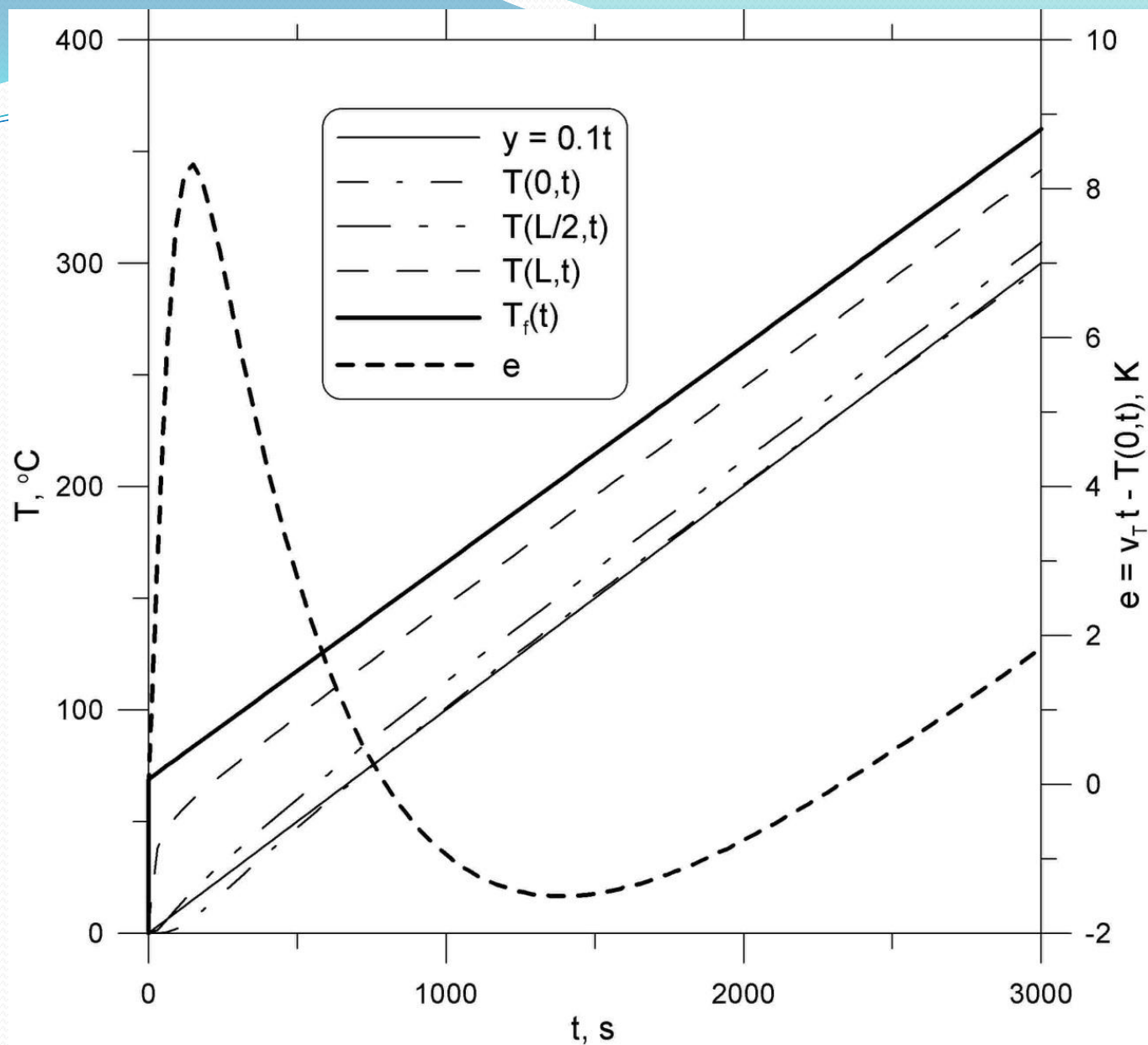
Fig.8b. Fluid and slab temperature changes when optimum fluid temperature changes are approximated by a ramp function; Δt = 30s.

Fig.8c. Fluid and slab temperature changes when optimum fluid temperature changes are approximated by a ramp function; $\Delta t = 60$s.
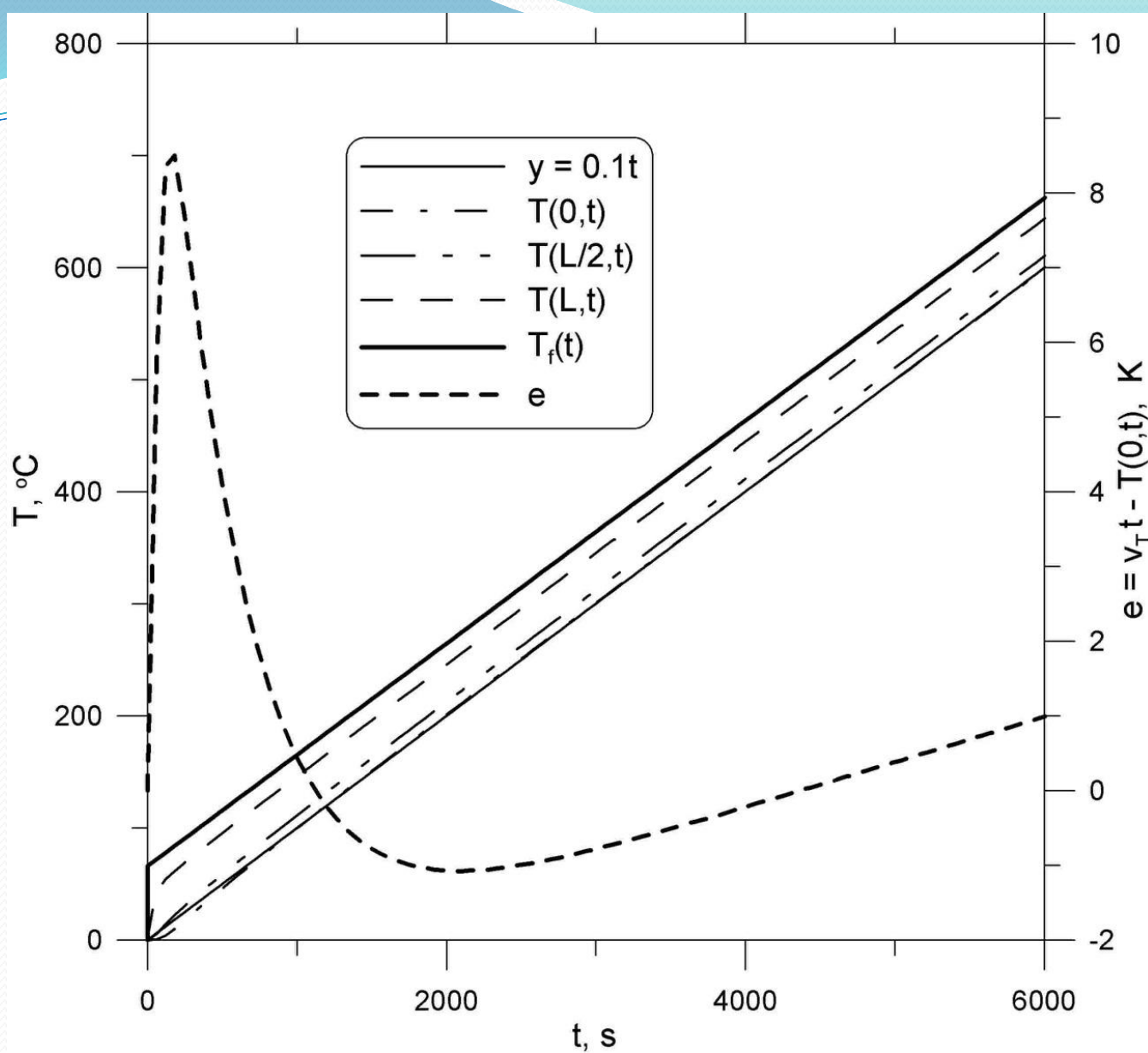
4. Examples of calculation of optimum fluid temperature with respect to thermal stresses

Firstly, the optimum medium temperature changes over time, during the heating of a plate, of the thickness H = 0.1 m will be determined. The edges of the infinitely large plate can expand freely, but they cannot bend. The following data was assumed for the calculations: the thermal conductivity: k = 41.1 W/(m·K), the specific heat: c = 532 J/(kg·K), the density: ρ = 7782 kg/m³, The Young modulus is E = 1.966·10¹¹ N/m², the linear thermal expansion coefficient b = 1.32·10⁻⁵ 1/K and the Poisson ratio n = 0.29. The heat transfer coefficient at the surface of the heated plate equals: h = 2000 W/(m²·K). The other surface of the plate is thermally insulated.
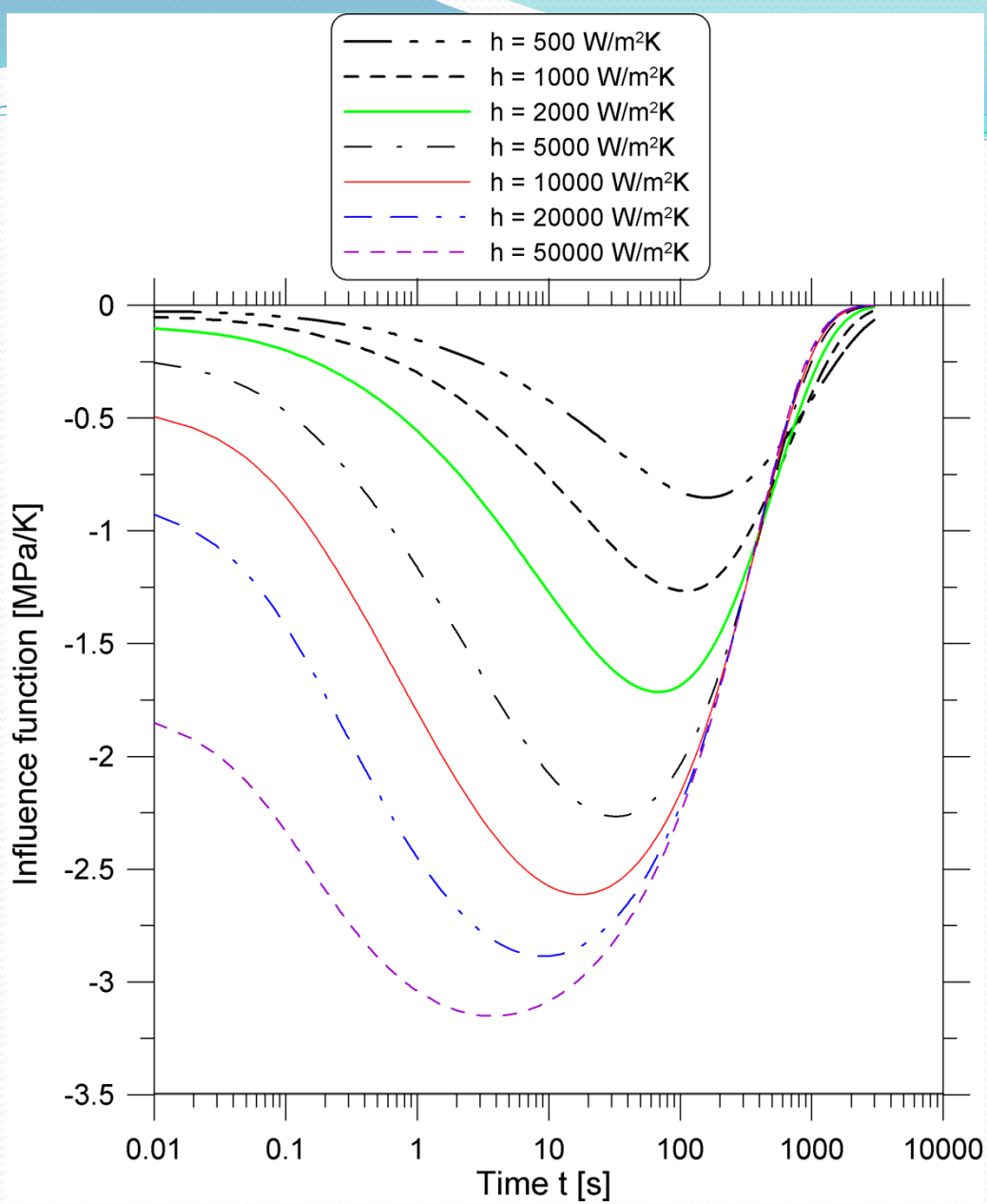
Fig. 9. Plot of the influence function for the 0.1 m thick plate

The allowable compressive stress on the heated surface of the plate is: $\breve{\sigma}_a$ = - 109.1 MPa. At the start time, the plate temperature is even and equals 0° C. The time changes of the influence function for various heat transfer coefficients are presented in Fig. 9. The time point, at which the influence function reaches the maximum absolute value, depends on the heat transfer coefficient. The greater the value of the heat transfer coefficient, the earlier will the absolute maximum value of the stress occur. The maximum absolute value of the influence function also increases with the increase of the value of the h coefficient. The optimum changes of the medium temperature are shown in Fig. 10.
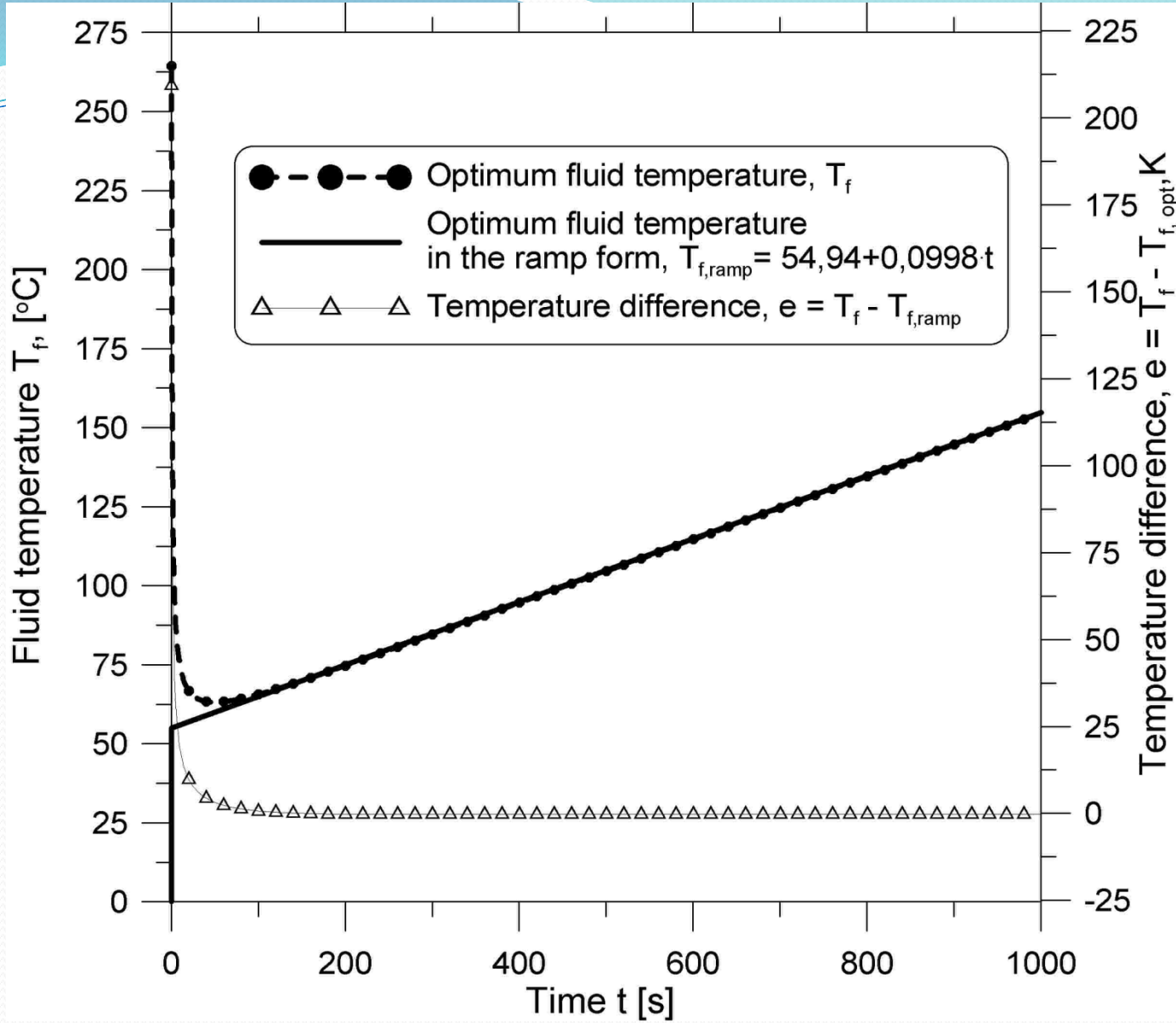
Fig. 10. Optimum medium temperature during the heating process of a thick walled plate

From the analysis of the results presented in Fig. 10 can be seen, that it is impossible to achieve the optimum medium temperature at the beginning of the heating process, because this temperature is very high. Thus, the optimum temperature was approximated, using a ramp function consisting of the step temperature rise at time $t = 0$ and a linear temperature increase for time $t > 0$. The value of the initial medium temperature jump and the rate of the linear medium temperature rise were determined using the least squares methods, in such a way that assures that the integral over time from the square of the difference between the actual stress and the allowable stress on the heated surface of the plate is minimised.

In the estimated optimum medium temperature $T_{f,ramp}$ = 54.94 + 0.0998 t time t is expressed in seconds. This optimum ramp heating can easily be conducted in power plants. The step increase of the medium temperature by 54.94 K can also be achieved without difficulty in real life by flooding the component with water at a temperature higher by 54.94 K than the initial temperature of the component.
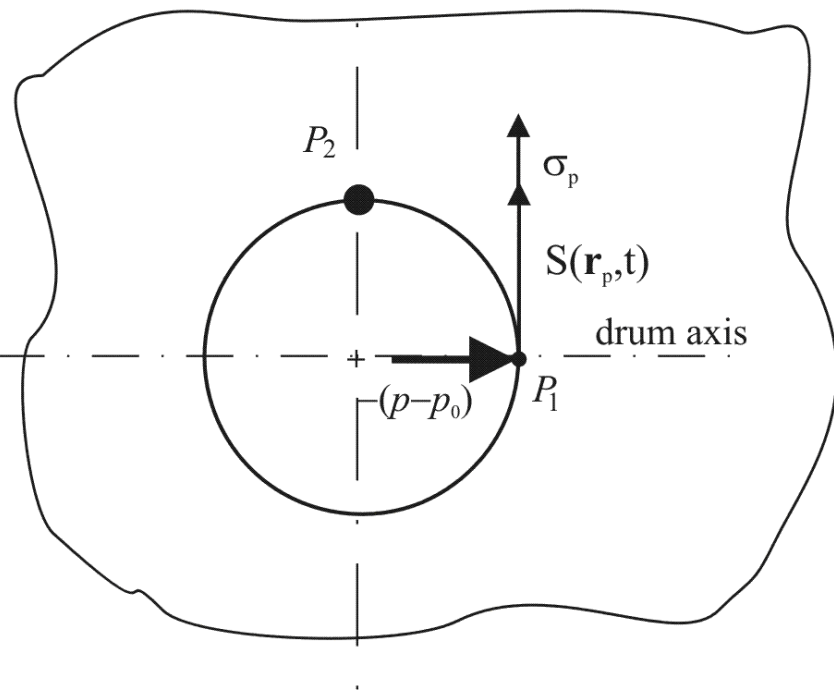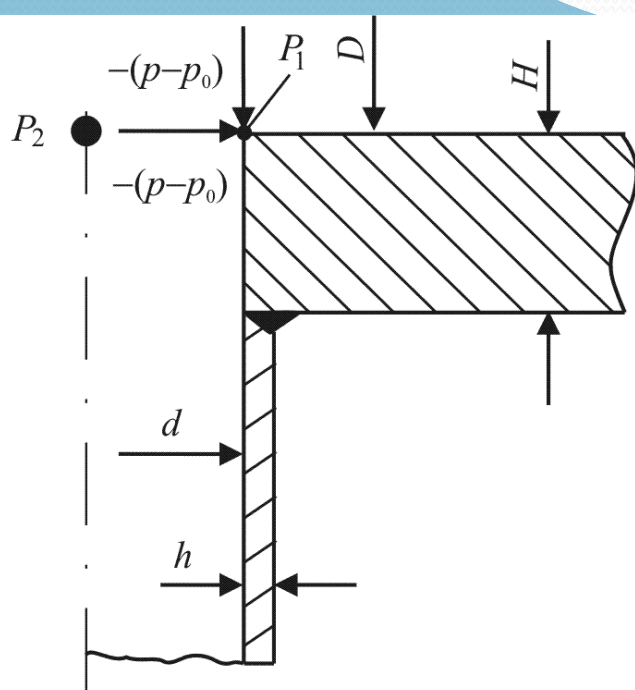
Fig. 11. Longitudinal section of the boiler drum – downcomer junction

In the second example, optimum water temperature changes will be determined with respect to total stress at the points P_1 and P_2 on the edge of the boiler drum-downcomer intersection. The following boiler drum dimensions were assumed for the calculation: D = 1.7m, d = 0.09m, H = 0.09m and h = 0.006m (Fig. 11). Also, the following properties of steel were assumed: k = 42 W/(m·K); c = 538.5 J/(kg·K); ρ = 7800 kg/m³; E =1 .96 10^{11} N/m²; β = 1.32 10^{-5} 1/K and v = 0.3. The heat transfer coefficient on the inner surface of the drum and downcomer is h = 1000W/(m²·K). The outer surfaces of the boiler drum-downcomer intersection are thermally insulated. The stress distribution analysis was done for the elastic state.

The stress concentration coefficients are: $\alpha_p = 2.65$ at the point P_1 and $\alpha_p = 0.51$ at the point P_2, respectively. Since the diameter and wall thickness of the downcomer tube is much smaller than the diameter and wall thickness of the boiler drum, the intersection resembles a plate with a hole subjected to biaxial stretching stresses with 2:1 ratio. For a plate with such a load, the stress concentration coefficient is 2.5 at the point P_1 and 0.5 at the point P_2. The thermal stress concentration coefficients in quasi-steady state are $\alpha_T = 1.86$ at the point P_1 and $\alpha_T = 2.074$ at the point P_2, respectively. Numerical model has been used for the determination of the influence function at points P_1 and P_2.

FEM analysis was carried out by means of the ANSYS software. The maximum absolute value of the function $u(\mathbf{r}, t)$ is larger at the point P_2 in comparison with its value at the point P_1. Since total compressive stresses at the point P_2 reach a larger value, the optimum medium temperature change rate with regard to circumferential stresses at point P_2 is smaller than the temperature change rate at point P_1. Furthermore, the temperature jump at the beginning of the process is smaller at the point P_2. If stresses at the point P_2 affect the course of heating and cooling, the start-up operation is longer, while shut-down lasts shorter in contrast to durations obtained by means of the approach, when P_1 is the criterion point.
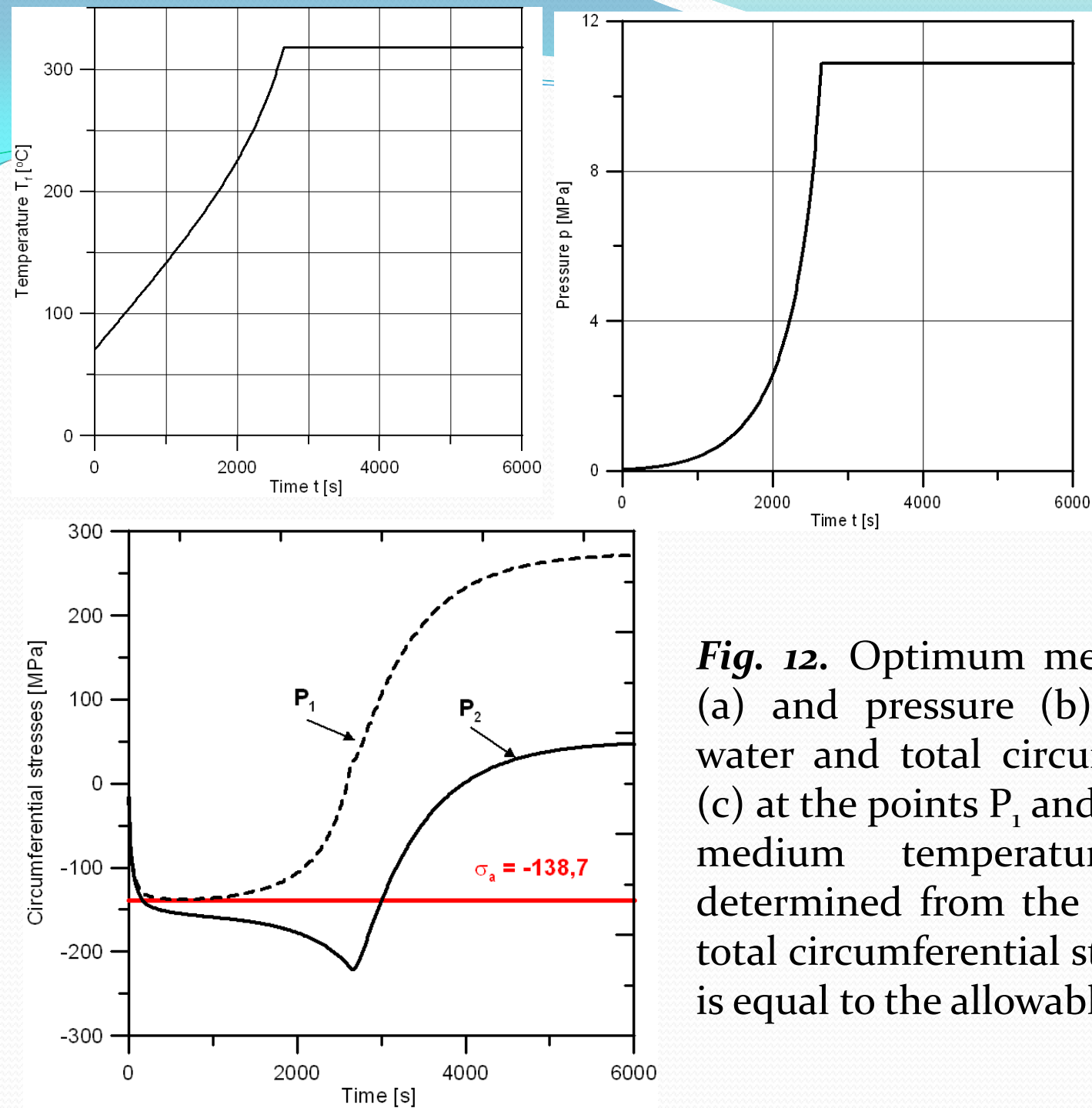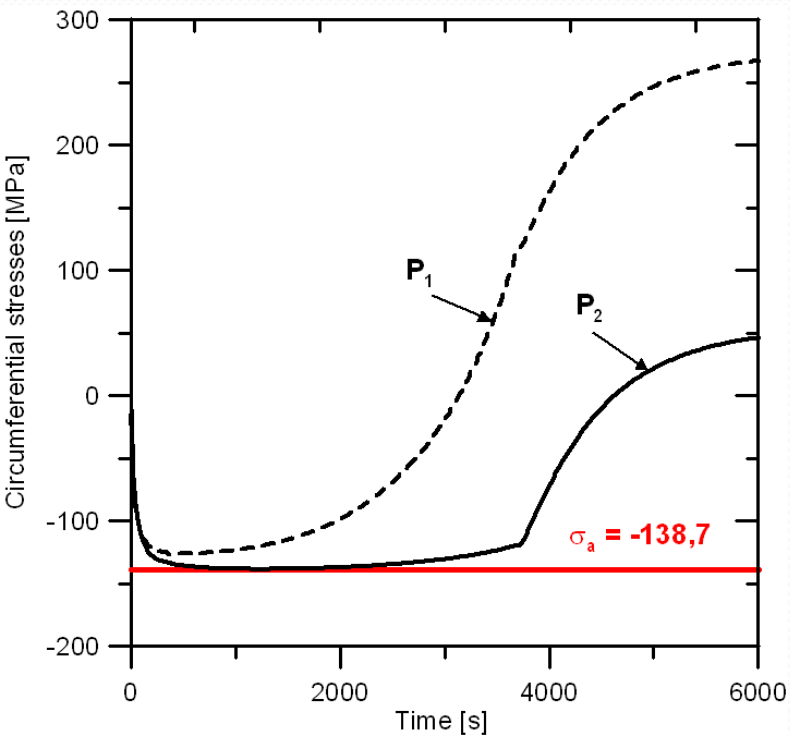
Fig. 12. Optimum medium temperature (a) and pressure (b) of the saturated water and total circumferential stresses (c) at the points P_1 and P_2 when optimum medium temperature changes are determined from the condition that the total circumferential stress at the point P_1 is equal to the allowable stress $\breve{\sigma}_a$
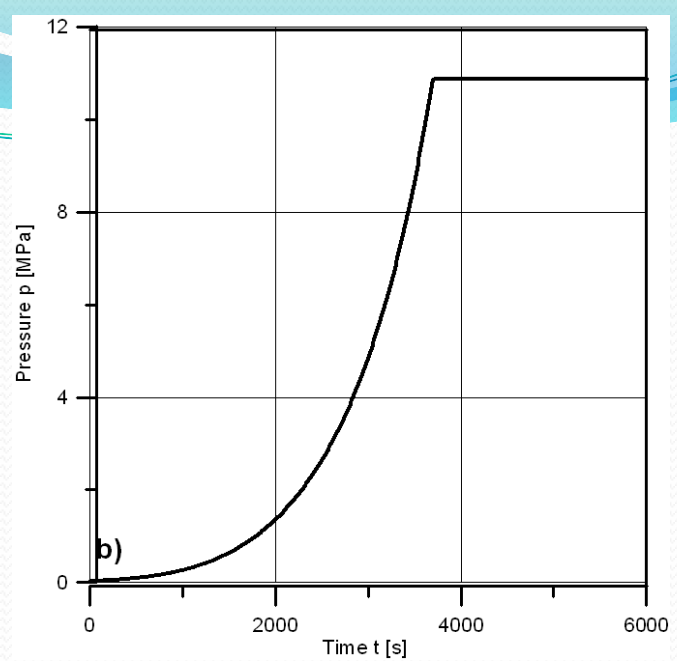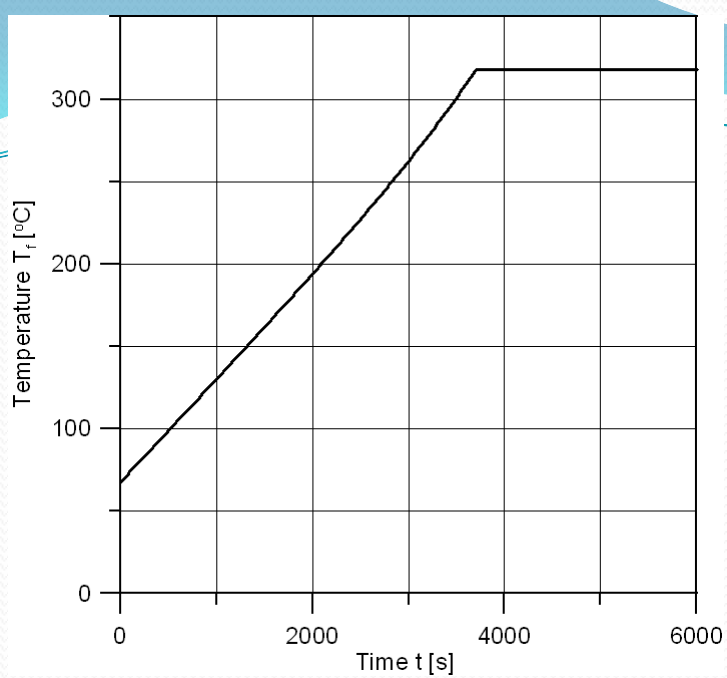
Fig. 13. Optimum medium temperature (a) and pressure (b) of the saturated water and total circumferential stresses (c) at the points P_1 and P_2 when optimum medium temperature changes are determined from the condition that the total circumferential stress at the point P_2 is equal to the allowable stress $\breve{\sigma}_a$

Next, the changes of total stresses, in conjunction with determined optimum temperatures, was determined by means of the 3D FEM analysis to check that total stresses do not exceed the allowable stresses. From the analysis of the results, one can see that allowable stresses are exceeded at the point P_2 (Fig 12c), when the optimum medium temperature is determined with respect to total stresses at point P_1 If the optimum heating and cooling of a boiler drum is carried out with respect to total stresses at the point P_2, the maximum stresses on the edge of a hole at the points P_1 and P_2 are smaller than the allowable stresses (Fig. 13c). It is advantageous when the boiler drum is heated with respect to stresses at the point P_2, since the allowable stresses both at the point P_1 and P_2 are not exceeded and the lifetime of the pressure component is longer.

4. Conclusions

Five different methods for predicting optimum temperature changes of the heating fluid were presented. The solutions based on the numerical approximation of the convolution integral compare favourably with other methods and can be used to determine the optimum fluid temperature with respect to the prescribed temperature or stress histories at the interior location. This method is appropriate for bodies with complex shapes. The influence function can be computed using the Finite Element Method.

The solution for the optimum temperature of the fluid obtained by using the Laplace Transform method is accurate, if the desired temperature history is prescribed at locations near the heated surface. The Burggraf method is inaccurate to predict optimum temperature changes in the early stages of heating. It requires an improvement of the inverse problem solution to account for the non-uniform temperature distribution resulting from the quasi-steady-state temperature distribution. The identical results to those obtained by the Burggraf method gives the space marching method. In the fifth method the optimum fluid temperature is approximated by an appropriate function of time and unknown parameters.

All the analyzed methods are not able to find an exact or accurate optimum fluid temperature changes at the beginning of the heating process.

The difficulties encountered in searching of the solution of the transient IHCP realize us, that we can find very often only very approximate solution.